UNIVERSITY OF CALIFORNIA SAN DIEGO

Protein Kinase G1 Activation Improves Diabetic Fracture Healing

A thesis submitted in partial satisfaction of the requirements for the degree Master of Science

in

Bioengineering

by

Julian Joseph Garcia

Committee in charge:

Professor Robert L Sah, Chair
Professor Renate B Pilz
Professor Lingyan Shi

2021

The thesis of Julian Joseph Garcia is approved, and it is acceptable in quality and form for publication on microfilm and electronically.

University of California San Diego

2021

TABLE OF CONTENTS

ACKNOWLEDGEMENTS

I would like to acknowledge Professor Robert Sah for his guidance not only throughout my master's program, but before the program even began. I have learned invaluable lessons with his systematic way of thinking, and his assistance in various projects has helped me become a better scientist.

I would also like to acknowledge Professor Renate Pilz for her guidance throughout my master's project. I have learned just as much with professor Pilz; she has been wonderful to work with even in the midst of a global pandemic.

I will be the first to say that 2020 was absolutely difficult as we all tried to navigate a global pandemic, not to mention social injustice in the US. Both Professor Sah and Professor Pilz have been extremely helpful, understanding, and encouraging in such a difficult time where personal life events added to, and began to overcome, my mental well-being. For this, I am forever indebted to them, and hope they both understand how they have been, and continue to be, such pivotal role models in my life.

I would also like to thank those that helped in the lab. Nadine Schall helped me get acquainted in the Pilz lab. Hema Kalyanamara always had words of encouragement and patience as I tried to absorb as much information from her intelligent mind as I could. Shyamsundar Pal-China helped with some animal work and was always a great person to work with in the lab. Dennis Zhuang for helping with various aspects of the study, and then always helping when I needed to find something. Finally, Van Wong, for helping in the many ways he did not only for the 3-point bending, but also in using other instruments in the lab.

Material from this thesis appears in “Schall N, Garcia JJ, et al. Protein kinase G1 regulates bone regeneration and rescues diabetic fracture healing. *JCI Insight.* 2020 May 7;5:e135355.” The thesis author was the primary investigator and author of this subset of material.

VITA

2016 Bachelor of Science, University of California San Diego

2021 Master of Science, University of California San Diego

PUBLICATIONS

Schall N, Garcia JJ, Kalyanaraman H, Pal-China S, Lee JJ, Sah RL, Pfeifer A, Pilz RB. Protein kinase G1 regulates bone regeneration and rescues diabetic fracture healing. *JCI Insight*. 2020;5(9):e135355

ABSTRACT OF THE THESIS

Protein Kinase G1 Activation Improves Diabetic Fracture Healing

by

Julian Joseph Garcia

Master of Science in Bioengineering

University of California San Diego, 2021

Professor Robert L Sah, Chair

Bone fractures are a major cause of morbidity and mortality, particularly in patients with diabetes, who have a high incidence of fractures and exhibit poor fracture healing. The NO/cGMP/protein kinase G (PKG) signaling pathway mediates osteoblast response to estrogens and mechanical stimulation, and is downregulated in diabetes by a defective enzyme, soluble guanylate cyclase (sGC). Here, we used a mouse mono-cortical defect model to stimulate bone regeneration in diabetic and non-diabetic mice which were treated with either vehicle or a NO-independent activator of oxidized sGC, cinaciguat. Diabetic mice demonstrated low *Vegfa* and *Bmp2/4* expression in bone and impaired bone regeneration after injury; notably, the cGMP-

elevating agent cinaciguat restored *Vegfa* and *Bmp2/4* expression, full bone healing, but had no effect on mechanical properties of uninjured bone in the diabetic animals, likely due to the short treatment duration. We conclude that PKG1 is a key orchestrator of VEGF and BMP signaling during bone regeneration and propose pharmacological PKG activation as a novel therapeutic approach to enhance fracture healing.

BACKGROUND

|The human skeleton is an integral structure that supports soft tissues and protects vital organs of the body. It may seem that bone is a stagnant tissue, however there is a constant interaction between bone cells that work to maintain homeostasis in the form of continuous remodeling. The outer surface of bone is made up of a thin layer called the periosteum where fibroblasts and periosteal progenitor cells can be found [Florencio-Silva, 2015]. The thicker layer covered by the periosteum is called compact, or cortical bone, and osteocytes, who can sense and respond to variations in mechanical stimulus, are embedded within the dense collagen matrix (Figure 1) [Florencio-Silva, 2015]. The inner lining of cortical bone, the endosteum, encapsulates the medullary cavity which is filled with bone marrow (Figure 1) [Biga].

There are four main types of bone cells that are constantly remodeling the bone matrix. Bone resorbing osteoclasts (Oc), activated by RANKL expression and derived from monocytes, bone laying osteoblasts (Ob), who produce soluble receptor osteoprotegerin (OPG) and are derived from bone marrow stromal cells, osteocytes that are responsible for mechanotransduction and bone lining cells that are thought to regulate bone remodeling on the endosteal surface (Figure 2) [Kalyanaraman, 2018]. Not only are these cells important for maintaining proper homeostasis, but they also play an important role in fracture repair.

Every year fractures occur at a high rate, in the US alone there are more than 15 million fractures, with poor bone quality contributing significantly to an increased risk [Hadjiagyrou, 2014]. Under normal conditions fracture repair occurs in a concerted series of events resulting in the total union of the damaged tissue. Immediately following a fracture, a hematoma and fibrin clot, filled with growth factors, inflammatory cytokines, and hormones forms at the site [Hadjiagyrou, 2014]. It is thought that signals which result from the injury such as, BMP, COX-2/PGE2, and Wnt/β-catenin are responsible for activating stem cell progenitors, in the periosteal

lining and bone marrow, to proliferate [Hadjiagyrou, 2014]. As progenitor cells are proliferating, migrating and accumulating at the injury site they are also concurrently differentiating into Ob's and chondrocytes [Hadjiagyrou, 2014]. Ob's and chondrocytes are matrix producing cells that are also responsible for producing signaling molecules that initiate the next stage of repair and maintain the healing process [Hadjiagyrou, 2014].

There are two forms of fracture healing that mimic stages in bone development, and can be simultaneously at work, intramembranous (primary) ossification and endochondral (secondary) ossification [Hadjiagyrou, 2014]. Under stable conditions, intramembranous (primary) ossification dominates where along the surface of the periosteum progenitor cells differentiate directly into Ob's that are then capable of directly laying down bone matrix [Hadjiagyrou, 2014]. In an unstable fracture, endochondral (secondary) ossification occurs where progenitor cells differentiate into chondrocytes that deposit a cartilaginous callus [Hadjiagyrou, 2014]. The soft cartilaginous callus forms in the more hypoxic region of the fracture, and the low oxygen tension in the callus activates hypoxia-related molecular pathways to stimulate angiogenesis and restore blood circulation [Hadjiagyrou, 2014]. The blood vessels can then supply chondroclasts and osteoprogenitor cells that remove calcified cartilage and differentiate into Ob's which can then lay bone matrix [Hadjiagyrou, 2014]. Once bone repair has completed the bone is fully restored to its original structure and function.

Unfortunately, 10% of fractures in the US develop complications in the healing process resulting in delayed healing, unfavorable anatomical positions, and non-union [Jiao, 2015]. Conditions such as diabetes, osteoporosis, and aging lead to reduced bone quality increasing your risk for developing a fracture [Kalyanaraman, 2018]. Diabetes accounts for a large portion of the 10% of improperly healed fractures [Jiao, 2015]. Diabetes mellitus is a metabolic disorder that,

with poor regulation, leads to high blood glucose levels. Under normal conditions insulin, produced by pancreatic β-cells, insulin binds to its receptor on the cell surface to initiate signaling cascades that aid in the uptake and metabolism of glucose [Jiao, 2015].

There are two types of diabetes, Insulin-dependent type I diabetes, or early onset, occurs where there is a destruction of insulin producing pancreatic β-cells leading to a decrease in insulin, ultimately resulting in high blood glucose levels [Jiao, 2015]. Then there is non-insulin dependent type II diabetes where cells do not respond to insulin effectively due to receptor insensitivity to insulin, and a reduction of insulin receptors on the cell surface, which also leads to an increase in blood glucose levels [Jiao, 2015]. Treatments for diabetes type I consist of monitoring blood glucose levels and administering insulin injections when glucose levels are imbalanced. When blood glucose is tightly regulated secondary effects from diabetes can be minimized, if not avoided. However, tight regulation can be tough to achieve, and hyperglycemia-induced oxidative stress has a detrimental effect on bone quality and fracture repair [Kalyanaraman, 2018].

Hyperglycemia causes oxidative stress through several mechanisms, "glucose auto-oxidation, nonenzymatic formation of advanced glycation end (AGE) products, increased mitochondrial superoxide (O_2^-) production, NADPH depletion from increased polyol pathway flux, and increased expression or activation of NADPH oxidase" [Kalyanaraman, 2018]. High blood glucose levels also increase flux through the hexosamine pathway which results in posttranslational *O*-linked modification of proteins [Kalyanaraman, 2018]. *O*-linked modifications decrease activity of nitric oxide synthase(s) (NOS); proteins that are responsible for producing a key signaling molecule, nitric oxide (NO) [Kalyanaraman, 2018].

NO is an important signaling molecule for most cellular and organ processes in the body, and plays a role in bone remodeling [Kalyanaraman, 2018]. There are several NOS isoforms

NOS1, NOS2, NOS3 and in the endothelial cells of diabetic patients NOS3 activity is found to be reduced [Kalyanaraman, 2018]. A reduction of NO in the serum and urine of diabetics indicates a systemic shortage of NO, which can have widespread effects [Kalyanaraman, 2018]. NO is a key signaling molecule for proper bone homeostasis, where NOS3 is the primary isoform expressed in bone [Kalyanaraman, 2018,6]. NO has several downstream targets with soluble guanylyl cyclase (sGC) being one [Kalyanaraman, 2018]. NO binds to an iron subunit of sGC activating the enzyme, sGC is then responsible for converting guanosine triphosphate (GTP) into cyclic guanosine monophosphate (cGMP), a signaling molecule that activates cGMP-dependent protein kinases (PKG1 and PKG2) (Figure 4) [Kalyanaraman, 2018]. However, when systemic levels of NO are decreased, such as in diabetes, cGMP concentrations also decrease [Kalyanaraman, 2018]. In addition to a reduction in systemic NO, sGC becomes deactivated in the presence of oxidative stress [Kalyanaraman, 2018]. The iron subunit of sGC becomes oxidized, then falls out of the enzyme rendering it inactive or with a reduced ability to convert GTP to cGMP [Kalyanaraman, 2018].

Osteoblast formation, differentiation, and function are severely impaired when sGC is inactivated, such as in diabetes [Kalyanaraman, 2018]. In addition, the presence of prolonged inflammatory cytokines such as TNF- **α**, induce and prolong osteoclast mediated resorption, and are thought to reduce osteoblast numbers through increased apoptosis [Jiao, 2015]. Increased AGEs in diabetes results in higher expression of RAGE (AGE receptors), and thus RAGE signaling, which activates transcription factor NF-κB to increase expression of RANKL [Jiao, 2015]. Overall increases in RANKL expression activate osteoclast mediated resorption. It is known that AGEs also inhibit Osteoblast differentiation and induce osteoblast apoptosis [Jiao,

2015]. Ultimately, Ob's are negatively affected in diabetes, but recent studies *in vitro,* and in mice, have shown promise in restoring osteoblast function using Cinaciguat [Kalyanaraman, 2018].

Recent work in the lab showed that cinaciguat, an NO-independent activator of sGC, restores proliferation and differentiation of preostoeblasts exposed to high glucose [Kalyanaraman, 2018, Erdmann, 2013]. Oxidative stress was also reduced in POBs treated with cinaciguat [Kalyanaraman, 2018]. In addition the effects of cinaciguat on type 1 diabetic mouse model [Kalyanaraman, 2018]. Mice were injected with streptozotocin and remained hyperglycemic for at least 2 weeks prior to starting treatment. Treatment with either vehicle, or cinaciguat lasted 4 weeks before euthanasia (Figure 5A) [Kalyanaraman, 2018]. Cinciguat was able to restore serum cGMP levels in diabetic mice back to control levels (Figure 5B) [Kalyanaraman, 2018]. Treatment also restored important bone quality measures as determined by μCT such as trabecular number (Tb.N) and trabecular bone volume (BV/TV) (Figure 5 C and D) [Kalyanaraman, 2018]. Osteoblast numbers were also restored whereas osteoclast counts were reduced in treated mice as compared to controls (Figure 5 E and F) [Kalyanaraman, 2018].

VEGF is responsible for mediating angiogenesis, and others have shown that NO donors increase basal VEGF mRNA in a cGMP-dependent dependent manner [Pilz, 2003]. Additionally, in a PKG1 osteoblast specific KO mouse *Vegfa* expression was reduced, and bone regeneration was impaired indicating a potential regulation of *Vegfa* by PKG1 [Schall, 2020]. Since previous work in the lab showed that NO and cGMP stimulate Ob function and that NO and cGMP regulate vasculogenesis we hypothesized that reconstituting the defective sGC signaling in diabetic bone would improve diabetic fracture healing.

METHODS

Study Design & Statistics

8-week-old mice were injected with either streptozotocin (STZ), to induce type 1 diabetes (T1DM), or vehicle. 14 days later tail vein blood was used to test blood glucose levels, where those that were 270 mg/dl, or greater, were considered to be hyperglycemic, and those that were injected with STZ but did not have a level greater than the threshold value were not used in the study. 28 days after injection of STZ a 0.8mm drill hole was placed in the anterior surface of the right tibia. On post-surgical days (PSD) 1-9 T1DM and non-T1DM mice were treated with either cinaciguat or vehicle. On PSD 10 mice were euthanized, and tissues were harvested. There were 4 different groups included in the study; (1) non-T1DM treated with vehicle, (2) non-T1DM treated with cinaciguat, (3) T1DM treated with vehicle, and (4) T1DM treated with cinaciguat. Since, in this study there were two variables (DM vs non-DM; Vehicle vs cinaciguat) A two-way ANOVA was used in all statistical analyses(Figure 6) [Schall, 2020].

Tibial monocortical defect model

Male 12-week-old mice were placed under general anesthesia by intraperitoneal injection of 100 mg/kg ketamine and 10 mg/kg xylazine. The lateral aspect of the right tibia was exposed, preserving the periosteum. An osseous hole (0.8 mm in diameter) was created through the anterior cortex of the tibia using a round burr attached to a dental drill (5000 rpm), with saline irrigation to remove bone fragments, as described previously [Hu, 2016]. The soft tissue wound was closed by separately suturing the muscle and skin layers with 4-0 absorbable gut suture. After surgery, mice received a subcutaneous injection of 0.1 mg/kg buprenorphine-SR (release over 72 hours) for analgesia. Mice were monitored daily; all mice were ambulating normally after awakening from anesthesia. Ten days after surgery, mice were euthanized by CO_2 intoxication and exsanguination.

The advantages of the drill hole model are that it is highly reproducible and does not require a metal fixation device, leading to fewer postsurgical complications compared with other fracture models with mechanical instability [Schall, 2020].

Generation of mice with type I diabetes

Male 8-week-old C57BL/6 mice from Envigo/Harlan were randomly divided into 4 groups: groups 1 and 2 (12 mice each) received streptozotocin at 100 mg/kg intraperitoneally for 2 days, while groups 3 and 4 (controls, 9 mice per group) received vehicle injections. Two weeks after the start of injections, glucose was measured in tail vein blood, and mice with a glucose concentration of more than 270 mg/dL were considered diabetic. Two weeks later mice underwent surgery for placement of the defect. One day postoperatively, the mice in groups 1 and 3 received vehicle and mice in groups 2 and 4 received cinaciguat at 10 μg/kg/d intraperitoneally for 9 days. On day 10, the mice were euthanized [Schall, 2020].

μCT

Ethanol-fixed tibiae were analyzed using a Skyscan 1076 scanner at 9-μm voxel size and applying an electrical potential of 50 kVp and a current of 200 mA, with a 0.5-mm aluminum filter. Mineral density was determined by calibration of images against 2-mm–diameter hydroxyapatite rods (0.25 and 0.75 g/cm^3). To measure regenerating bone, the VOI in the drill hole region was defined as a cylinder with a diameter of 0.65 mm (74 pixels) and a height of 0.3 mm (33 slices), extending from the outer surface of the tibia through the cortical bone. Bone defects containing cortical bone fragments greater than 100 μm in the long axis were excluded from analysis. Three-dimensional images from the VOI were constructed using CTvol software. A global threshold (70–255) was chosen to identify trabecular bone in the defect area [Schall, 2020].

Histology

For histological analysis of regenerating bone, paraffin-embedded tibiae with monocortical defects were sectioned sagittally and stained with Masson's trichrome. An area of 200 μm × 600 μm between the 2 cortical bone ends of the defect was analyzed (a 0.12-mm^2 "region of interest"). Only sections showing a fully intact region of interest were analyzed. Collagen content (percentage of the area of interest stained by aniline blue) was measured using Nanozoomer Digital Pathology NDP.view2 software [Schall, 2020].

qRT-PCR

After removing growth plates and bone marrow, bone shafts were snap-frozen in liquid N_2 and pulverized. RNA was purified from bone shafts and POBs, and qRT-PCR was performed with 300 ng of total RNA as described [Kalyanaraman, 2017]. All primers were tested with serial cDNA dilutions. Relative changes in mRNA expression were analyzed with 18S rRNA serving as an internal reference; the mean ΔCt obtained for control mice was used to calculate the fold change in mRNA expression in diabetic mice using the $2^{-\Delta\Delta Ct}$ method [Schall, 2020].

3-Point Bending

The mechanical properties of femurs adjacent to the defect (right femur) were tested to failure using a three-point-bending test on a Biomomentum V500cs (Biomomentum, Laval, Ontario, Canada) mahine [Turner, 1993]. Femurs adjacent to the defect were excised from mice on the day of euthanasia, and all soft tissue was peeled off using a kim wipe. Femurs were then stored at -20℃, wrapped in PBS soaked kimwipes until used in testing. Before testing, they were thawed at room temperature; moisture was maintained by soaking in PBS until ready for testing. Femurs were positioned horizontally on two supports separated 6mm's with the anterior surface pointing upwards(Figure 14A). The loading force was directed vertically at the midshaft of the bone at a

displacement rate of 0.16 mm/s; load and displacement was recorded for each femur(Figure 14C). Stiffness was extrapolated by taking the slope between 20-50% of max load (most linear region) on the load-displacement curve and max load was determined at the peak of the curve.

RESULTS

|Previous work in the lab demonstrated that NO and cGMP stimulates osteoblast function and that NO and cGMP regulate vasculogenesis [Kalyanaraman, 2018]. It was also shown that cinaciguat, a NO-independent activator of soluble guanylyl cyclase, can activate protein kinase G to improve osteoblast function in diabetic osteoporosis (Figure 5 B-D) [Kalyanaraman, 2018]. Therefore, it was hypothesized that cinaciguat might also improve bone fracture healing in mice with type I diabetes (T1DM). Streptozotocin (STZ) was administered to 8-week-old male C57BL/6 mice, to induce type I diabetes. 14 days following the injection of STZ, blood glucose levels were tested using tail vein blood. 28 days after STZ injection, after mice had been hyperglycemic for at least two weeks, a 0.8 mm mono-cortical hole was placed in the anterior surface of the right tibia (Figure 6B). On postsurgical day (PSD) 1, daily injections of cinaciguat, or vehicle were given until euthanasia on PSD 10 (Figure 6A). 10μg/kg/d doses of cinaciguat were administered since it was previously shown that this dose increased serum cGMP concentrations in diabetic animals to normal levels without affecting normal systolic blood pressure [Kalyanaraman, 2018]. In this study two non-T1DM groups and two T1DM groups were used that were either treated with cinaciguat, or vehicle for PSDs 1-9 and then euthanized on PSD 10 (Figure 6A and C).

Blood glucose levels (BGL) were tested using tail vein blood at 10 wks and 14 wks, and those that were injected with STZ and tested >270 mg/dl were considered to be diabetic while those mice below the threshold were not used in the study (Figure 7A). Mice that were diabetic lost on average 15% of their body weight compared with the nondiabetic controls, and treatment with cinaciguat had no effect on the weight of control or diabetic mice, and on blood glucose levels in either groups(Figure 7 A and B) [Schall, 2020].

Following euthanasia, defect bones (right tibias) were harvested from all mice and scanned using a skyscan 1076 computed tomography scanner. Once scanned reconstructed bones were

rotated in a data viewing software to show the defect (Figure 8A). Once rotated, a volume of interest (VOI) was determined. A cylinder was placed in the center of the 0.8 mm drill hole and extended from the outer cortical surface of the tibia through the cortical hole region (Figure 8 B and C). The VOI cylinder had a diameter of 0.65 μm and a depth of about 330 μm into the medullary cavity (Figure 8D). Micro-CT bone parameters were then measured using the volume described. VOI's which contained displaced cortical bone fragments larger than 100 um in length were excluded because these fragments, introduced at the time of surgery, could serve as small islands of bone matrix that would be expected to improve bone regeneration similar to a bone graft. Bone regeneration was severely impaired in diabetic mice as compared to control mice, with increased trabecular spacing and lowered trabecular number, bone volume per total volume (BV/TV) and bone mineral density (BMD) in the defect (Figure 9 B and C, Figure 10 B and C). Cinaciguat also improved these parameters in the regenerating bone in control, non-diabetic mice.

Sagittal sections of the right tibia (defect bone) were stained using masson's trichrome stain, where collagen fibers stain blue, nuclei stain purple and muscle, cytoplasm and keratin stain red. Blue stained collagen within a predefined 0.12 mm^2 region of interest (ROI) was outlined and the area of collagen per area of ROI was quantified (Figure A, C, and D). Collagen content was significantly decreased in diabetic mice when compared with controls, and treatment with cinaciguat restored collagen deposition in diabetic mice. Cinaciguat did not have an effect on control mice.

The same histological sections used in quantifying collagen were also used to count Ob's, and osteoclast numbers. Small, single nuclei, and collagen lining cells were counted as Ob's. Ob's that were separated 5-10 μm from collagen surfaces, were only counted if there was visible osteoid between the collagen and cell (Figure 12B). Large multinucleated, bone lining, magenta cells were

counted as Oc's (Figure 12B). Osteoblast numbers were significantly decreased in diabetic mice compared to controls while Oc's were not different (Figure 12 C and D). Cinaciguat, however improved osteoblast numbers, but did not have an effect on osteoclast counts in either diabetic, or control mice (Figure 12 C and D).

Diabetic mice demonstrated decreased *Vegfa, Bmpr2,* and, *Bmp2/4* mRNA expression in non-injured tibial shafts as compared to controls. However cinaciguat restored expression of all 4 genes, consistent with its ability to increase serum *cGMP* concentration and its capacity to restore cGMP/PKG signaling in mice with STZ-induced diabetes [Kalyanaraman, 2018]. Expression of *Bmpr1* and *Hprt* was not affected in diabetic or control mice (figure 13 A and B).

Mechanical properties of the right femur were determined using a 3-point-bending test where bones were loaded till failure (Figure 14 A). Stiffness and max load were both decreased in diabetic bones when compared to controls, however cinaciguat had no effect on stiffness or max load in either controls or diabetics (Figure C and D).

DISCUSSION

|Diabetic patients not only have an increased risk of fracture, but also have a reduced ability to heal, which often contributes to complications [Jiao, 2015]. Endothelial nitric oxide synthases (eNOS) are downregulated resulting in lower systemic cGMP in patients with diabetes, and in mice with type I diabetes (T1DM) [Kalyanaraman, 2018]. Ob's that are under conditions of high glucose experience impaired NO/cGMP signaling due to O-Glc_N-acetylation of NO synthase-3 and oxidative inhibition of soluble guanylyl cyclase [Kalyanaraman, 2018]. *Vegfa*, *Bmp2/4*, and *Bmpr2* mRNA was found to be in low amounts in the bones of diabetic mice, and treatment with cinaciguat caused an increase of expression of these genes, which was consistent with cGMP/PKG1 regulation of *Vegfa* and *Bmp2/4* mRNA in Ob's, which was shown previously in the lab (Figure 13 A and B) [Schall, 2020,5]. Impaired wound healing in diabetics has been associated with a decrease in VEGF expression, therefore we hypothesized that impaired osteoblastic VEGF synthesis in diabetic bone may also contribute to poor fracture healing and activation of guanylate cyclase by cinaciguat may improve bone regeneration [Schall, 2020].

Bone regeneration was not only restored in diabetic mice, but also improved in control mice. This can indicate that stimulation of VEGF and BMP synthesis may have other applications than only improving bone regeneration in diabetics [Schall, 2020]. Patients with a low capability to initiate angiogenesis can also benefit from treatment with cinaciguat [Schall, 2020].

μCT bone parameters including cortical thickness were improved in a diabetic osteoporosis mouse model, where mice were treated with cinaciguat for 4 weeks [Kalyanaraman, 2018]. Although the femurs of diabetic mice showed a decrease in stiffness and max load, treatment with cinaciguat had no effect. This may indicate that treatment with cinaciguat for 10 days is not sufficient to improve systemic bone mechanical properties. A longer duration of treatment may be necessary to see a response in systemic mechanical properties.

Primary ossification occurs when progenitor cells differentiate directly into Ob' and then proceed to deposit bone matrix [Hadjiagyrou, 2014]. Primary ossification dominates when the fracture site is stable, while secondary ossification occurs when the fracture is unstable [Hadjiagyrou, 2014]. For this study a monocortical defect model was used where the fracture site was stable. Therefore, the effects of PKG1 stimulation in diabetes on callus formation, and secondary ossification was not examined [Schall, 2020]. In future studies, the effects of PKG1 stimulation on diabetic fracture healing using an unstable fracture model could be investigated.

Currently, the only application of bone morphogenetic proteins (BMPs) is by locally administering them at the time of fracture [Dai, 2015]. Although BMPs are essential at improving bone regeneration, dosing, and delivery in a clinical setting has proven to be quite difficult [Dai, 2015]. Abnormal bone formation is often a problem since there is rapid release of high doses at the fracture site [Hettiaratchi, 2020]. Results in *Prgk1* OB-KO mice have shown that the positive effects of cGMP on bone regeneration are mediated by PKG1 via regulation of *VEGF* and *BMP* signaling [Schall, 2020]. Currently, some cGMP-elevating pharmacological agents in clinical use are NO-generating nitrates, phosphodiesterase-5 inhibitors, and soluble guanylyl cyclase stimulators, unlike the preceding agents, cinaciguat activates soluble guanylyl cyclase in an NO-independent manner [Schall, 2020]. Oxidative stress that is present in diabetes results in a soluble guanylyl cyclase enzyme that has a reduced capacity to respond to NO, however cinaciguat is capable of activating the oxidized version of the enzyme [Kalyanaraman, 2018]. cGMP elevating agents, such as cinaciguat, could be a novel treatment for patients with impaired fracture healing [Schall, 2020]. Patients that have a reduced ability to initiate angiogenesis may benefit the most from cGMP elevating agents [Schall, 2020].

REFERNCES

[1] Armour KE, Armour KJ, Gallagher ME, Godecke A, Helfrich MH, Reid DM, Ralston SH. Defective bone formation and anabolic response to exogenous estrogen in mice with targeted disruption of endothelial nitric oxide synthase. *Endocrinology.* 2001 Feb; 142:760-6

[2] Biga LM, Dawson S, Harwell A, Hopkins R, Kaufmann, LeMaster M, Matern P, Morrison-Graham K, Quick D, and Runyeon J. Anatomy & Physiology. OpenStax/Oregon State University.

[3] Dai J, Li L, Jiang C, Wang C, Chen H, Chai Y. Bone morphogenetic protein for the healing of tibial fracture: a meta-analysis of randomized controlled trials. *PLoS One.* 2015 Oct 28;10:e0141670

[4] Erdmann E, Semigran MJ, Nieminen MS, Gheorghiade M, Agrawal R, Mitrovic V, Mebazaa A. Cinaciguat, a soluble guanylate cyclase activator, unloads the heart but also causes hypotension in acute decompensated heart failure. *Eur Heart J*. 2012 Jul 9; 34:57-67.

[5] Florencio-Silva, Rodrigues da Silva Sasso G, Sasso-Cerri E, Simoes MJ, Cerri PS. Biology of bone tissue: structure, function, and factors that influence bone cells. *Biomed Res Int*. 2015 Jul 13;2015:421746.

[6] Hadjiagyrou M, O'Keefe RJ. The convergence of fracture repair and stem cells: interplay of genes, aging, environmental factors and disease. *J Bone Miner Res* 2014 Nov; 29:2307-22

[7] Hettiaratchi MH, Krishnan L, Rouse T, Chou C, McDevitt TC, Guldberg RE. Heparin-mediated delivery of bone morphogenetic protein-2 improves spatial localization of bone regeneration. *Sci.* 2020 Jan 3;6:eaay1240

[8] Hu K, Olsen BR. Osteoblast-derived VEGF regulates osteoblast differentiation and bone formation during bone repair. *J Clin Invest.* 2016 Jan 5;126:509-26

[9] Jiao H, Xiao E, Graves DT. Diabetes and its effect on bone and fracture healing. *Curr Osteoporous Rep.* 2015 Oct;13:327-35.

[10] Kalyanaraman H, Ramdani G, Joshua J, Schall N, Boss GR, Cory E, Sah RL, Casteel DE, Pilz RB. A novel, direct NO donor regulates osteoblast and osteoclast functions and increases bone mass in ovariectomized mice. *J Bone Miner Res.* 2016 Sep 7;32:46-59.

[11] Kalyanaraman H, Schall N, Pilz RB. Nitric oxide and cyclic GMP functions in bone. *Nitric Oxide*. 2018 Mar 14;76:62-70

[12] Kalyanaraman H, Schwaerzer G, Ramdani G, Castillo F, Scott BT, Dillman W, Sah RL, Casteel DE, Pilz RB. Protein kinase G activation reverses oxidative stress and restores osteoblast function and bone formation in male mice with type I diabetes. *Diabetes.* 2018 Jan 4;67:607-23

[13] Pilz RB, Casteel DE. Regulation of gene expression by cyclic GMP. *Circ Res*. 2003 Nov 28;93:1034-46

[14] Schall N, Garcia JJ, Kalyanaraman H, Pal China S, Lee JJ, Sah RL, Pfeifer A, Pilz RB. Protein kinase G1 regulates bone regeneration and rescues diabetic fracture healing. *JCI Insight.* 2020 May 7;5:e135355

[15] Turner CH, Burr DB: Basic biomechanical measurements of bone: a tutorial. *Bone* 1993 Jul-Aug; 14:595-608.

[16] Wang W, Yeung K. Bone grafts and biomaterials substitutes for bone defect repair: A review. *Bioact Mat.* 2017 Jun 7;2:224-47

FIGURES

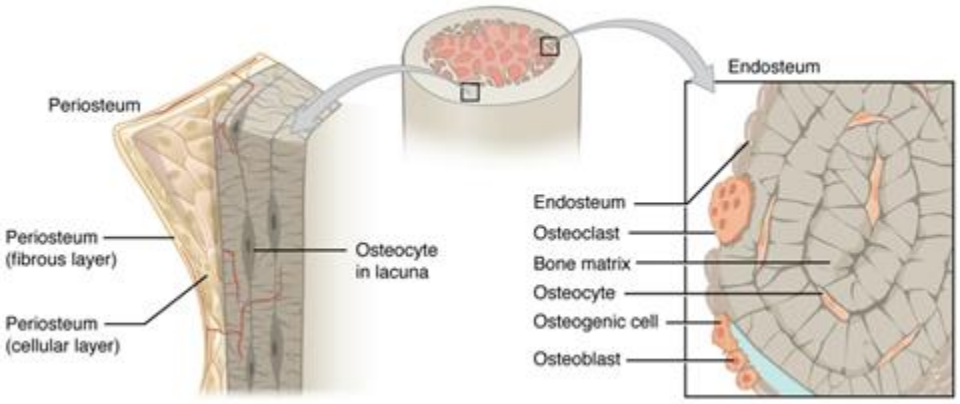

Figure 1: Layers of bone. The outer layer is a thin sheet of fibrous-like tissue called the periosteum where periosteal progenitor cells live. The periosteum covers a more dense cortical bone that encapsulates osteocytes. The inner surface of the cortical bone is called the endosteum where osteoblasts, osteoclasts and bone lining cells can be found [Biga].

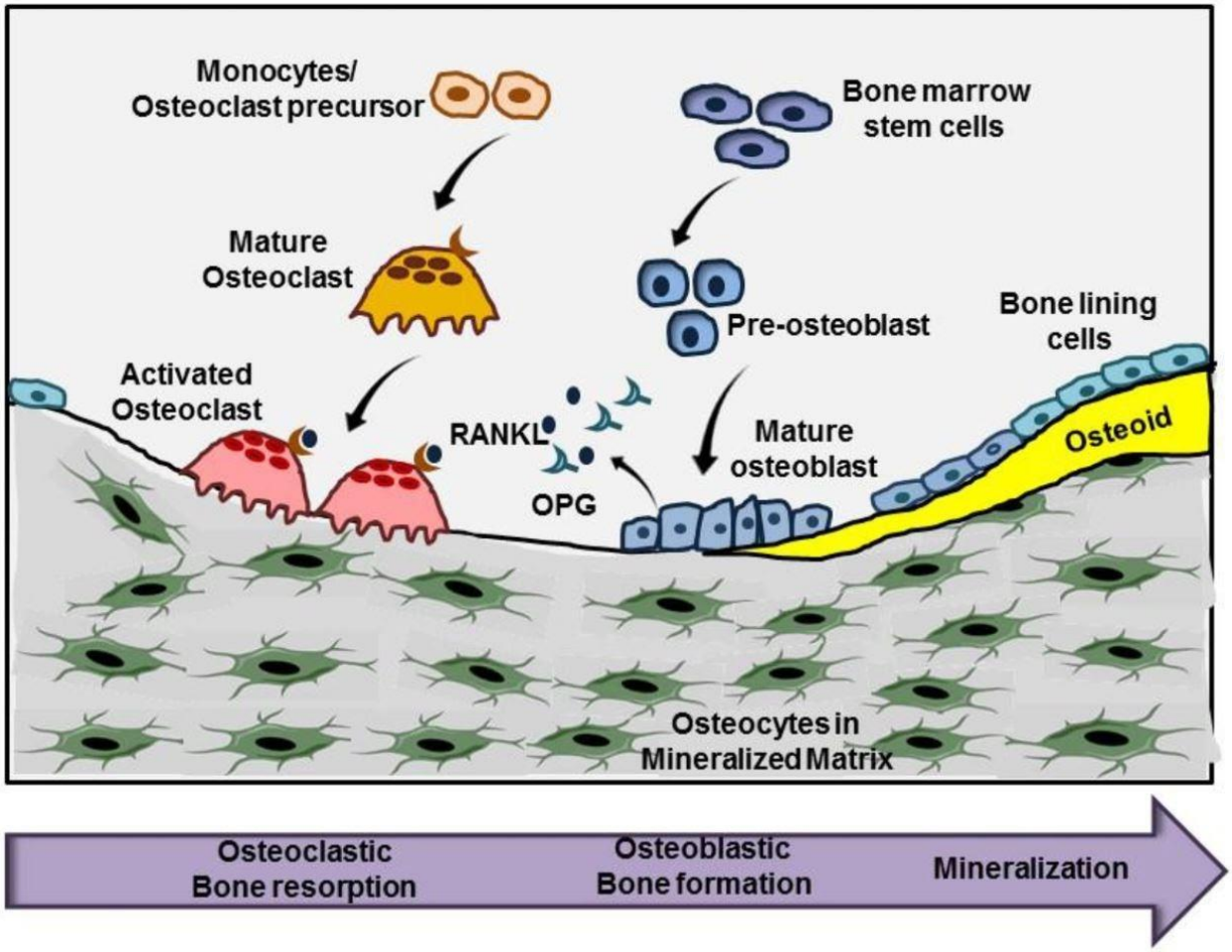

Figure 2: Bone cells. There are four main types of bone cells: bone resorbing osteoclasts, activated by RANKL expression and derived from monocytes, bone laying osteoblasts who produce soluble receptor osteoprotegerin and are derived from bone marrow stromal cells, osteocytes that are important in mechanotransduction and bone lining cells [Kalyanaraman, 2018].

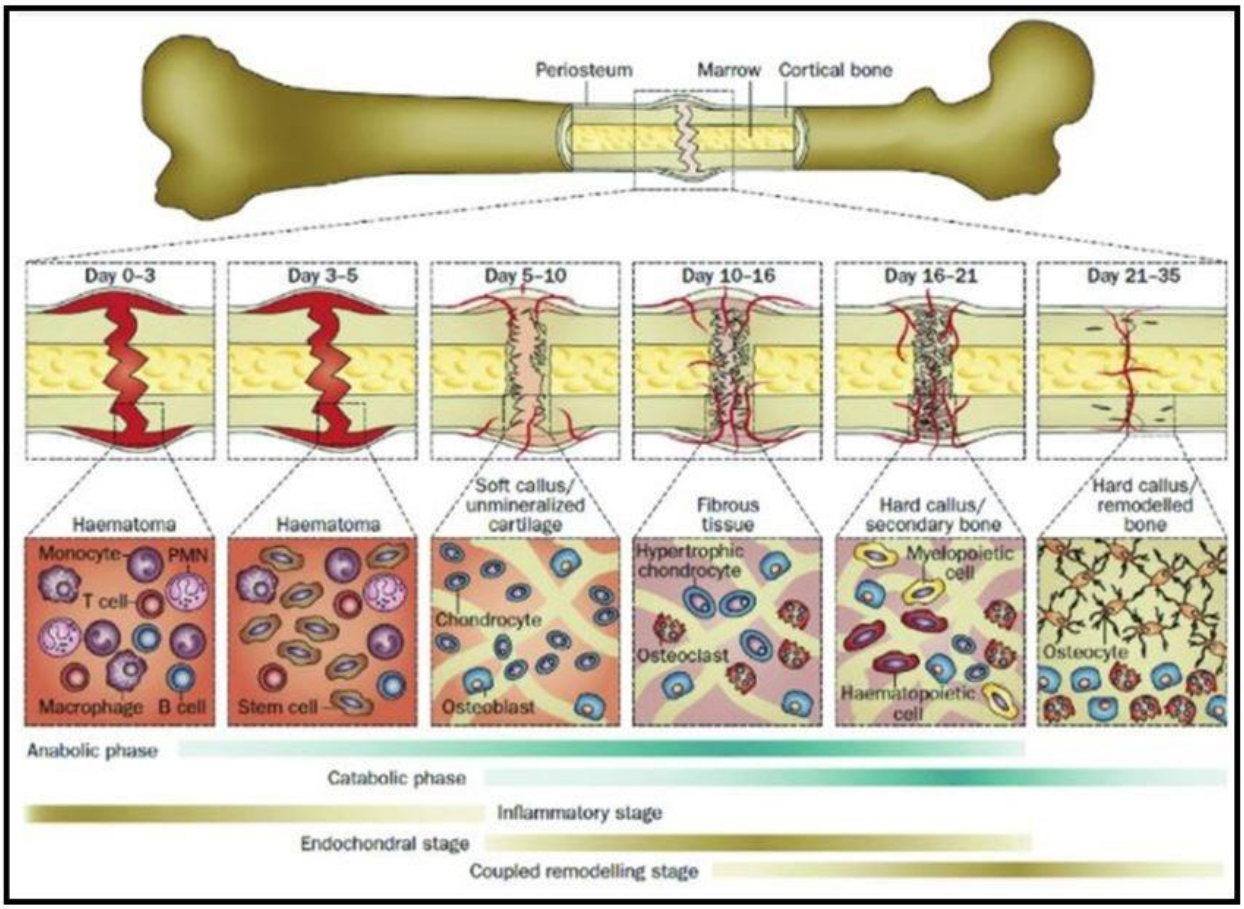

Figure 3: Fracture repair in healthy individuals. First the formation of a hematoma that is filled with growth factors, hormones and inflammatory cytokines that are responsible for initiating the repair response. These signaling molecules stimulate progenitor cell recruitment, proliferation, and differentiation into osteoblasts and chondrocytes. Depending on the stability of the fracture site either intramembranous (primary), or endochondral (secondary) ossification occurs and complete union of the defect occurs [Wang, 2017].

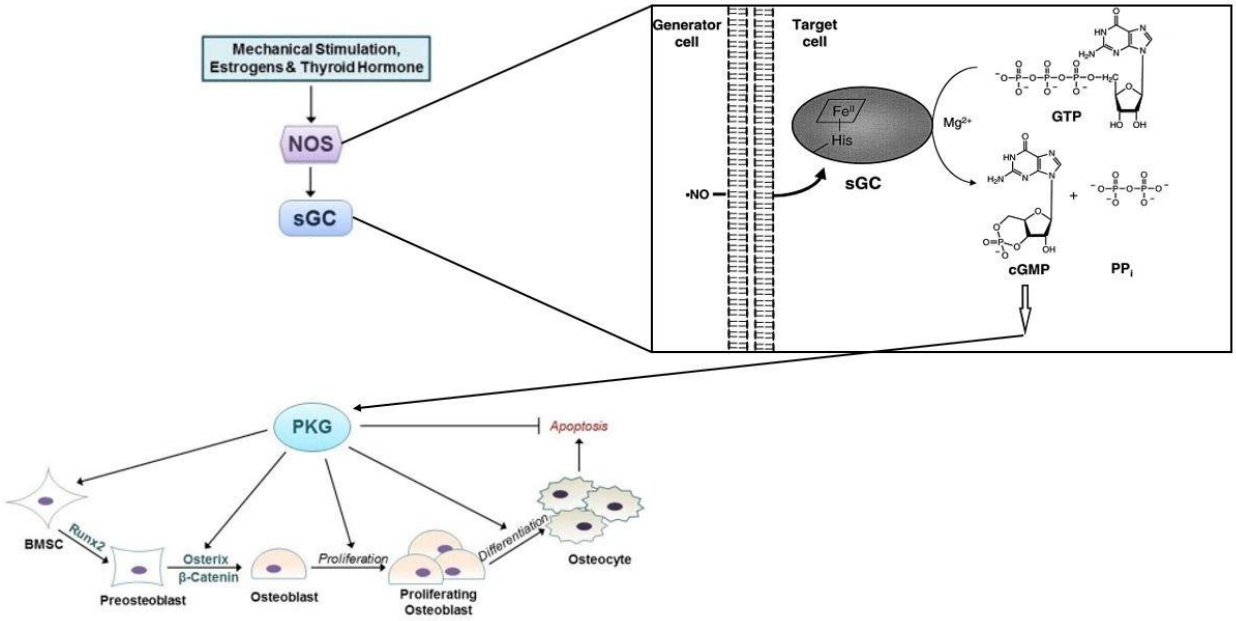

Figure 4: The NO/cGMP/PKG pathway in bone remodeling. In response to mechanical stimulus, estrogens and the thyroid hormone nitric oxide synthases produce nitric oxide (NO) which then enters the target cell. Inside the target cell NO activates soluble guanylyl cyclase (sGC) by binding to the iron subunit, initiating the conversion of GTP to cGMP. cGMP then signals the PKG family of proteins that contribute to the formation, proliferation and differentiation of osteoblasts[6].

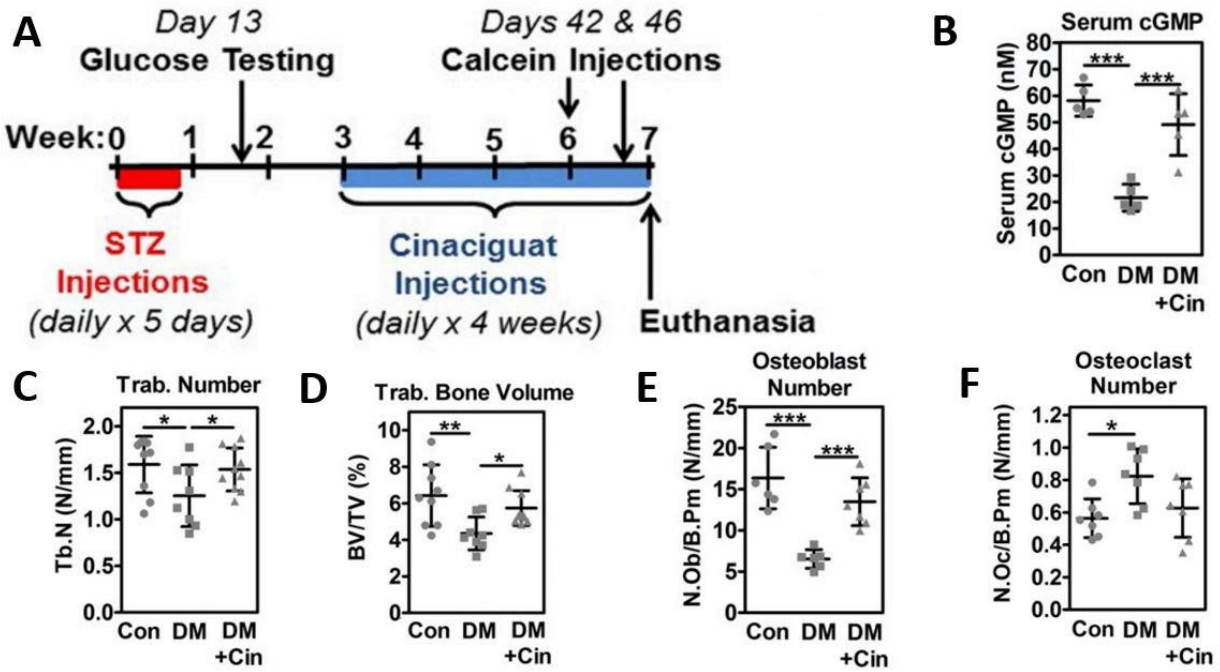

Figure 5: Cinaciguat effects in diabetic mice: increased serum cGMP**,** improved bone microarchitecture and bone formation, and reduced resorption. (A) Male C57BL/6 mice (12 weeks old) were treated with vehicle (Con) or injected with streptozotocin (STZ; 40 mg/kg/day i.p.) for 5 days. Blood glucose was measured 13 days after the start of injections, and STZ-administered mice that were hyperglycemic (>270 mg/dl) received vehicle (0.1% DMSO; DM) or cinaciguat (10µg/kg/day i.p.; DM+Cin) for 4 weeks starting 21 days after the start of STZ injections. At 7 and 4 days before euthanasia, the mice received calcein (25 mg/kg i.p.). (B) Serum cGMP concentrations were measured by ELISA 1h after the last cinaciguat injection. (C) trabecular number, (D) trabecular bone volume, (F) were measured by µCT analysis. (E) Osteoblasts (Ob) and (F) Osteoclasts (Oc) were counted on trabecular bone surfaces. B.Pm, bone perimeter; N., number. (*n* = 5-7 mice/group, except *n* = 8-10 mice/group for panels *D-F.) *P< 0.05, **P<0.01, ***P< 0.001* for the indicated comparisons (by ANOVA) [Kalyanaraman, 2018].

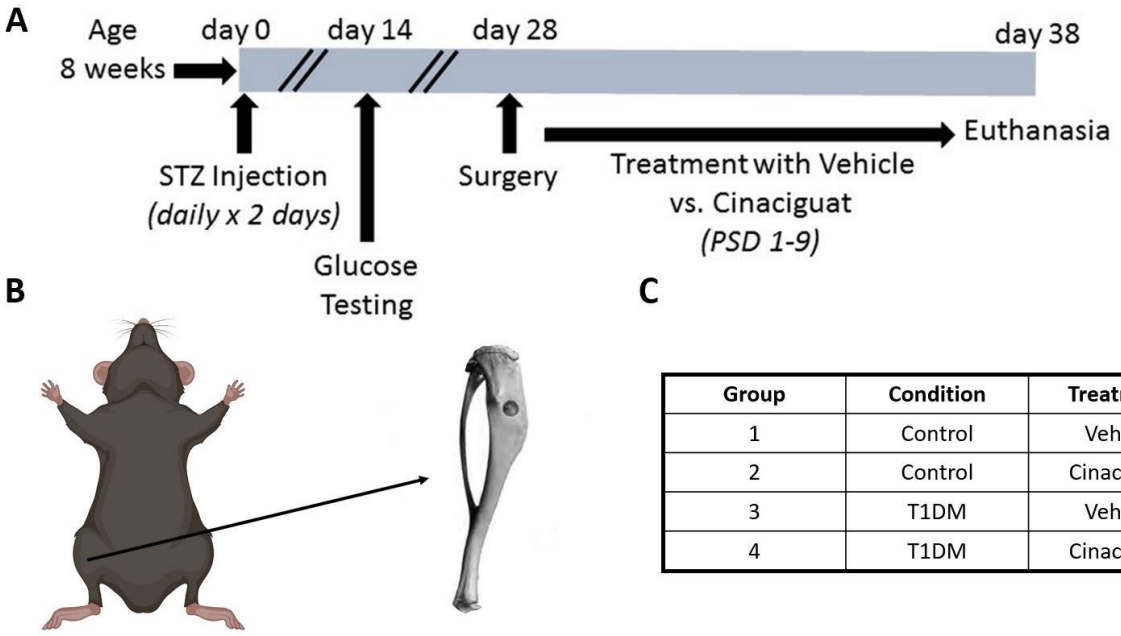

Group	Condition	Treatment
1	Control	Vehicle
2	Control	Cinaciguat
3	T1DM	Vehicle
4	T1DM	Cinaciguat

Figure 6: Study design. (A) Male mice, 8 weeks old, received vehicle (Control) and diabetic mice received streptozotocin (STZ) to induce type I diabetes. 14 days later blood glucose levels were tested using tail vein blood (>290 mg/dl were considered diabetic). 28 days following STZ injection (B) a 0.8-mm burr hole was surgically placed on the anterior surface of the right tibia in all mice. On postsurgical days (PSD) 1-9, mice were given daily intraperitoneal injections of either vehicle or cinaciguat (10ug/kg/d), and they were euthanized on PSD 10. (C) Study groups.

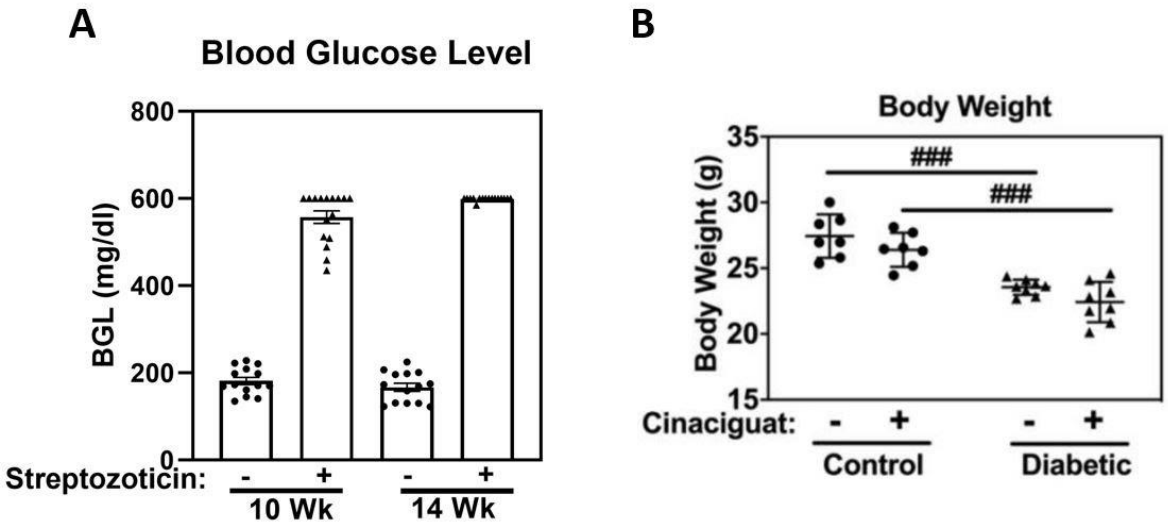

Figure 7: *In Vivo,* Health Measures. (A) Blood glucose concentrations (mg/dl) were tested from tail vein blood 2 weeks after STZ (10 wks) and on the day of euthanasia (14 wk). (B) The body weight of control and diabetic mice were measured on the day of euthanasia (age 14 wks). ###$p<0.001$ for comparison by 2-way ANOVA

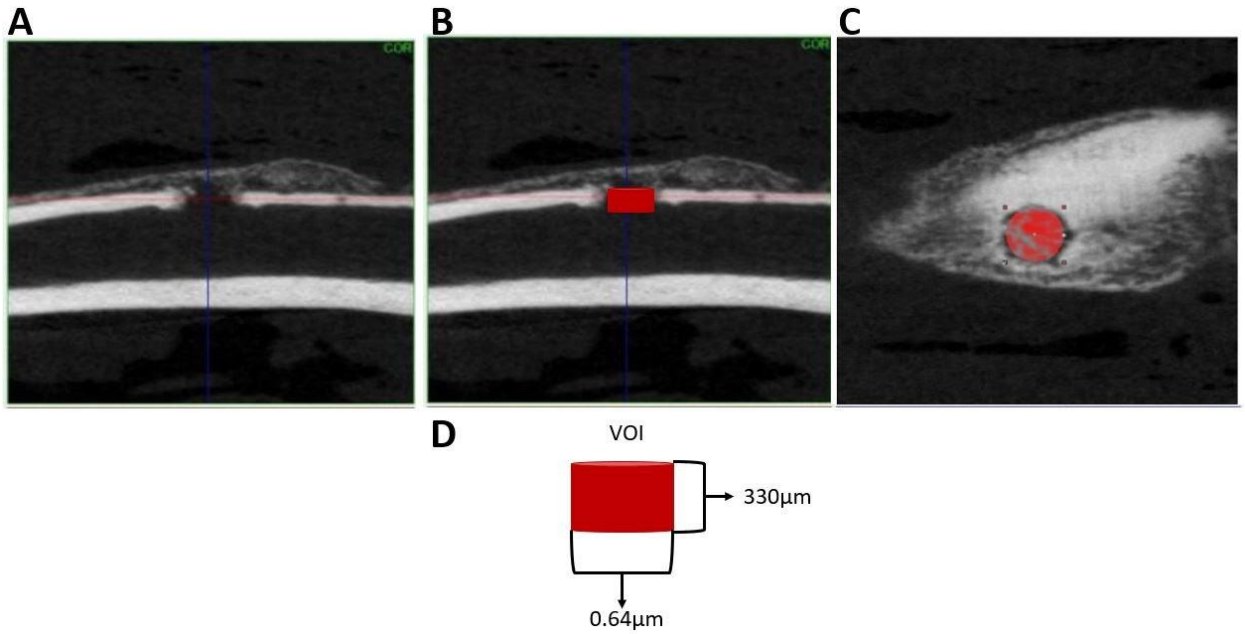

Figure 8: Determining the volume of interest. (A) Sagittal section of the right tibia showing the cortical bone. (B) Volume of interest (VOI) for micro-CT analysis.(D)The VOI was defined as a cylinder with a diameter of 0.65 mm (74 pixels) in the center of the drill hole, and with a height of 0.3mm (33 slices) , extending from the outer cortical surface of the tibia through the cortical hole region. (C) Top view of the cylindrical VOI shown in red. This transaxial view shows the anterior surface of the proximal tibia, with the 0.65 mm diameter (in red) placed in the center of the burr hole.

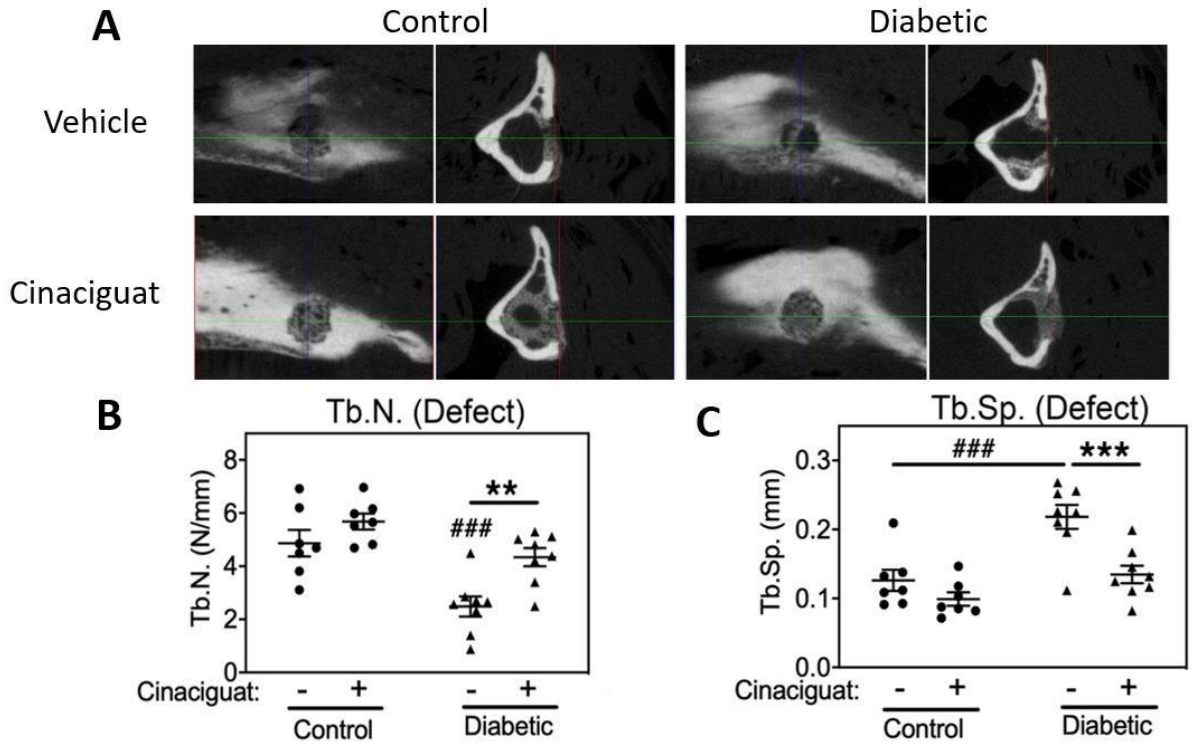

Figure 9: Tibia defect transaxial and transverse views, Trabecular number and spacing. (A) Transaxial and transverse views show regenerating bone within the defect volume of interest. (B) The trabecular number (Tb.N) and (C) trabecular spacing (Tb.Sp) were determined using CtAN image processing software where (n = 7 mice in each of the control groups, and n = 8 mice in each of the diabetic groups). ###$p<0.001$ and ***$p<0.001$ for comparison by 2-way ANOVA.

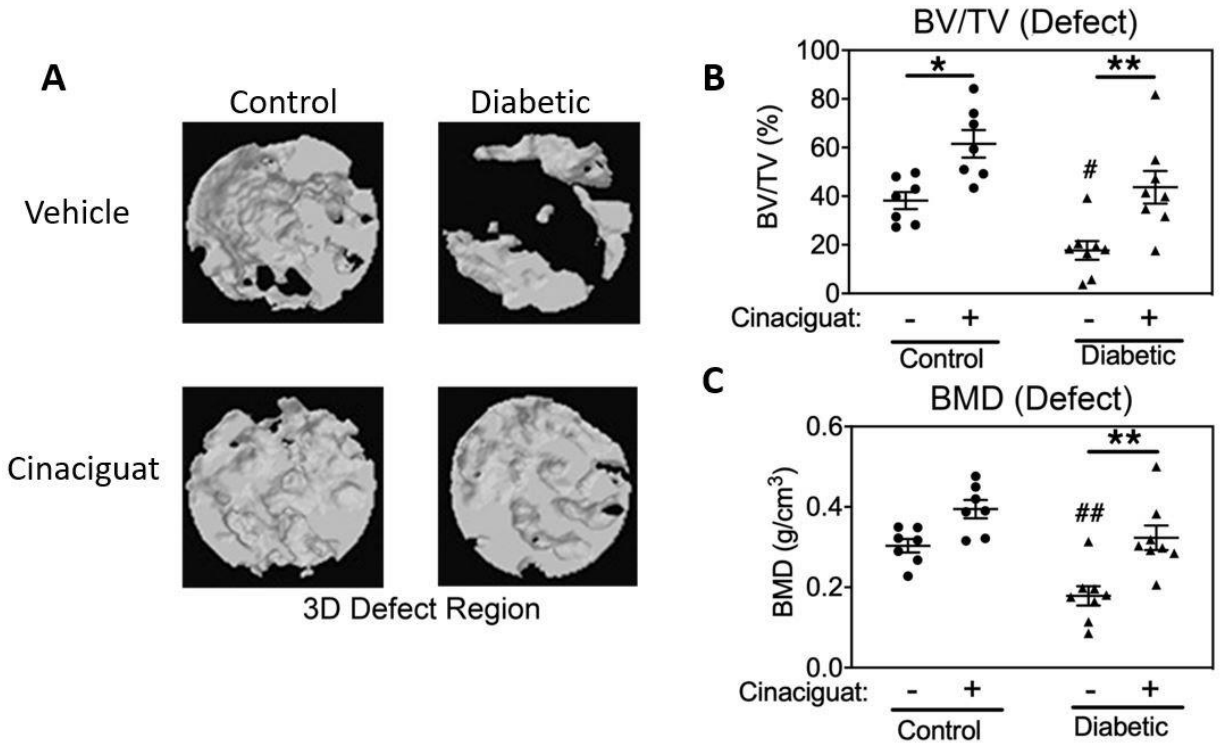

Figure 10: 3D reconstructed views of regenerating bone within the defect. (A) Anterior surface views of the defect VOI showing differences in bone mineral density and bone volume within the volume analyzed. (B) The bone volume per total volume (BV/TV), and (C) Bone Mineral Density (BMD) were analyzed by ctAN software analysis (n = 7 mice in each of the control groups, and n = 8 mice in each of the diabetic groups). *$p < 0.05$ and **$p < 0.01$ for indicated comparison by 2-way ANOVA.

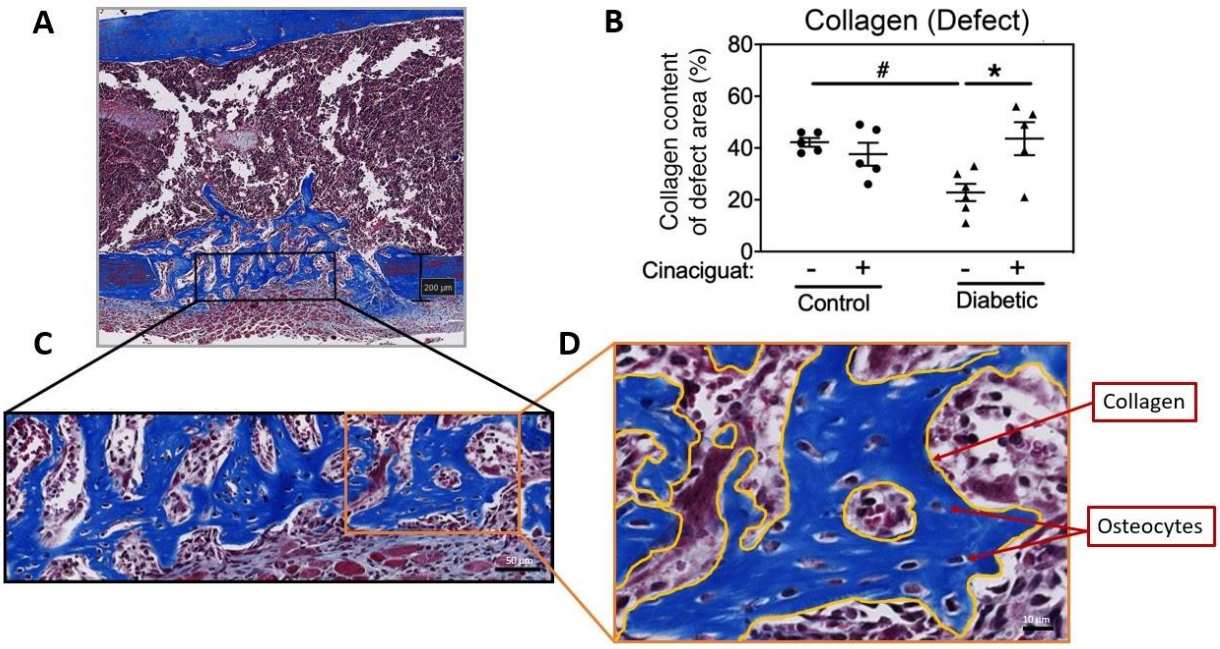

Figure 11: Collagen content. Collagen stained blue in a Masson's Trichrome stain was measured on bone sections in the 0.12 mm^2 "region of interest" within the defect of the injured tibiae (n=5-6 mice per group). #$p < 0.05$ and *$p < 0.05$ for comparison by 2-way ANOVA.

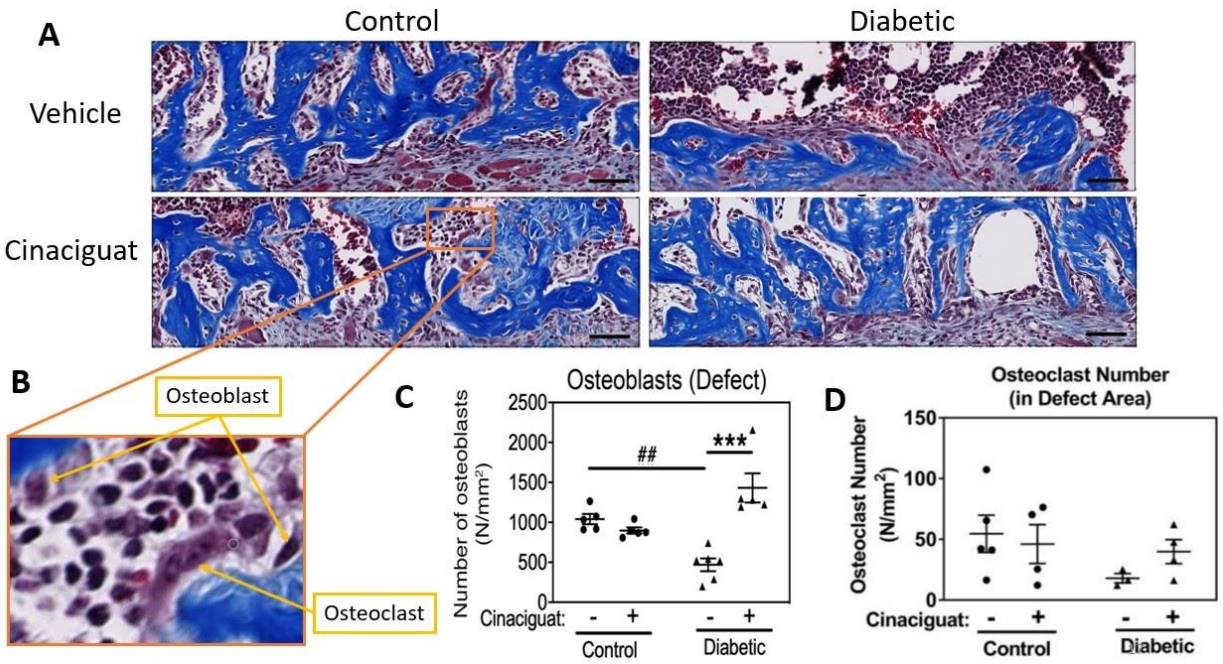

Figure 12: Osteoblasts and osteoclast counts. Osteoblast counts in trichrome stained sections within the 0.12 mm^2 "region of interest" on injured tibiae. (A) representative images of each group. (B) examples of osteoblasts (Ob) and osteoclasts (Oc) attached to collagen surfaces within the ROI. (C,D) Ob and Oc numbers counted per bone surface area (n=5-6 mice per group). ##$p < 0.01$ and ***$p < 0.001$ for comparison by 2-way ANOVA.

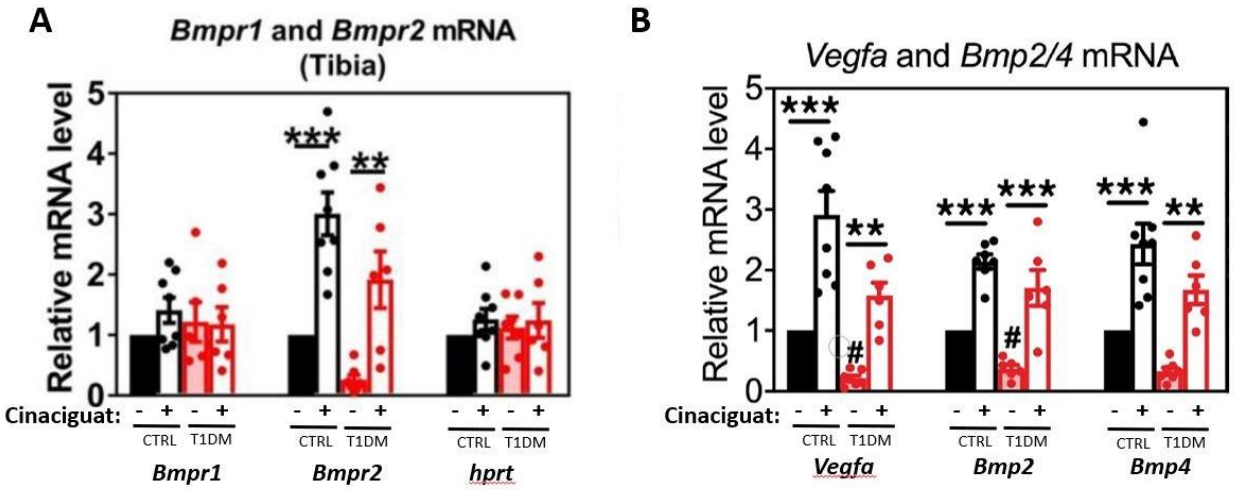

Figure 13: RT-qPCR of contralateral tibiae. (A) *Bmpr1*, *Bmpr2*, and *hprt* mRNA, (B) *Vegfa*, *Bmp2*, and *Bmp4* mRNAs were quantified by qRT-PCR in tibiae of control and diabetic mice treated with vehicle or cinaciguat (Cin); mRNA amounts were normalized to 18S rRNA, and the mean mRNA level found in tibiae of vehicle-treated control mice was assigned a value of 1 (n=6-7 mice per group). **p < 0.01 and *** p < 0.001 for the comparison by 2-way ANOVA.

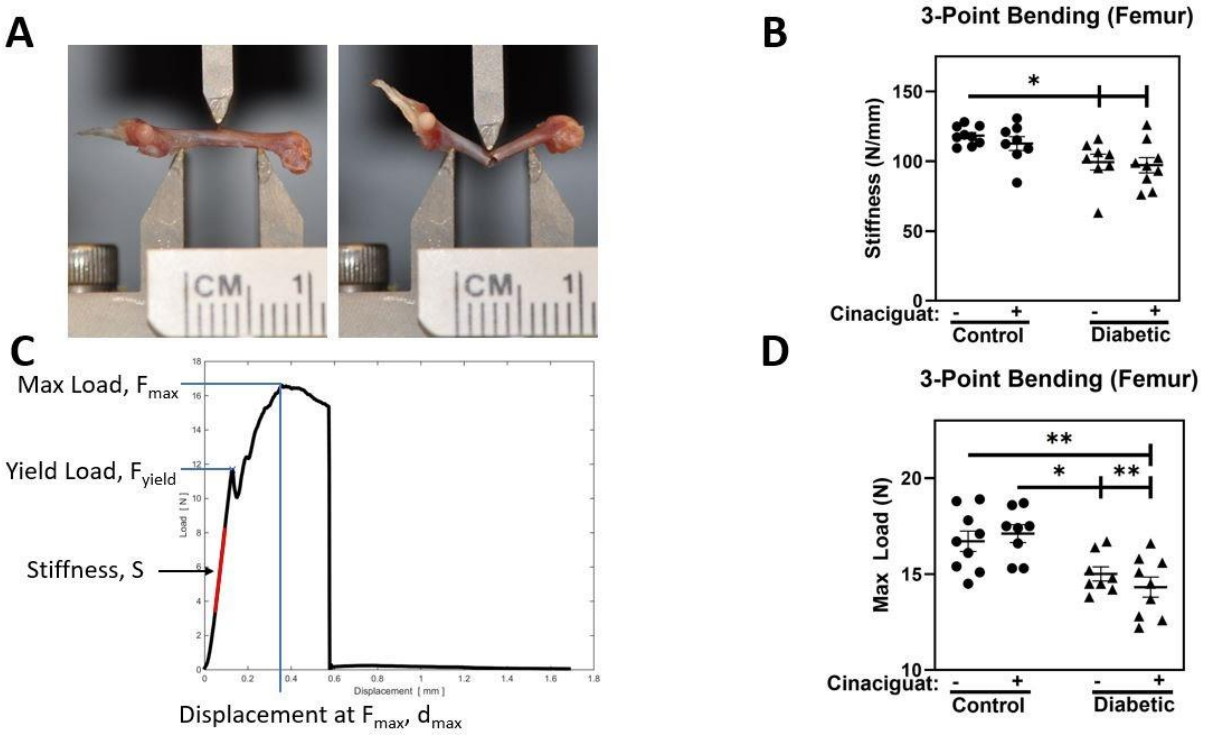

Figure 14: Stiffness, and max load values of femur. (A) Femurs were positioned horizontally on two supports separated 6mm with the anterior surface pointing upwards. (B) Stiffness extrapolated from the slope between 20-50% max load (C) Load vs displacement curve showing location of stiffness and max load. (D) Max load values of femur compared for control and diabetic mice treated with cinaciguat or not treated. *$p < 0.05$, and **$p < 0.01$ as compared in 2-way ANOVA.

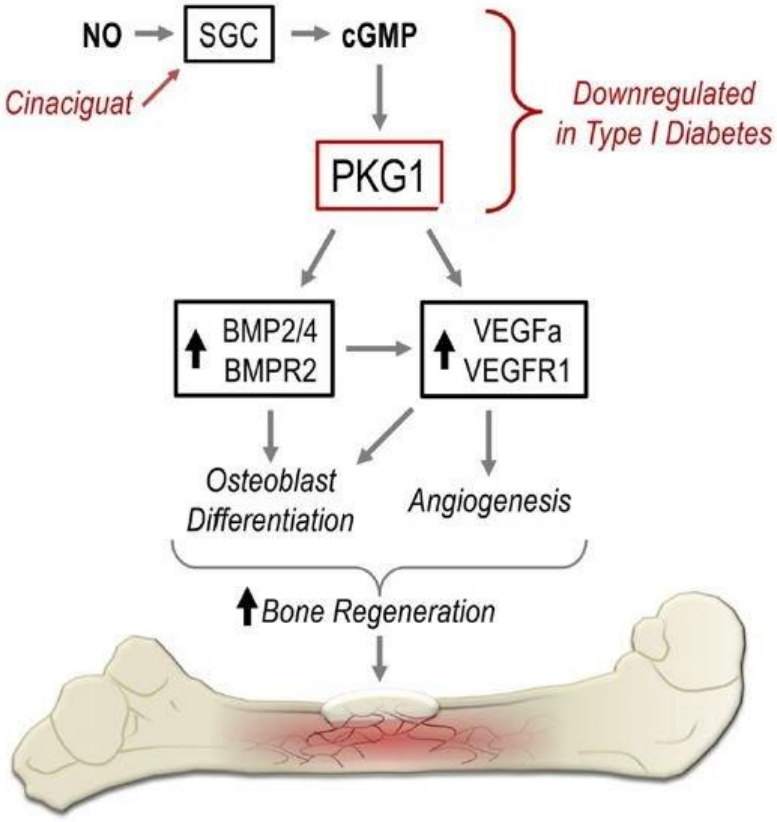

Figure 15. PKG1 regulation of bone regeneration via BMP and VEGF. Soluble guanylyl cyclase (sGC) generates cGMP in response to NO (or stimulation by cinaciguat) to activate PKG1, which in turn increases expression of *Bmp2/4*, *Vegfa*, and their receptors *Bmpr2* and *Vegfr1* in osteoblasts. BMP and VEGF are known to control osteoblast differentiation and angiogenesis and are crucial for all phases of fracture repair. Downregulation of NO/cGMP/PKG signaling in diabetic osteoblasts leads to impaired bone regeneration, but NO-independent sGC stimulation by cinaciguat in diabetic mice rescues fracture healing.

Material from this thesis appears in "Schall N, Garcia JJ, et al. Protein kinase G1 regulates bone regeneration and rescues diabetic fracture healing. *JCI Insight.* 2020 May 7;5:e135355." The thesis author was the primary investigator and author of this subset of material.